Thermal Model of High-Speed Spindle Units

Igor Alexeevich Zverev
Department of Machine Tools, Moscow State University of Technology (STANKIN)
In-Ung Eun
Department of Die & Mold Design, Kyonggi Institute of Technology
Won Jee Chung, Choon Man Lee*
Machine Tool Research Center, Changwon National University, #9 Sarimdong Changwon, Kyungnam, 641-773 Korea

For the purpose to facilitate development of high-speed spindle units (SUs) running on rolling bearings, we have developed a beam element model, algorithms, and software for computer analysis of thermal characteristics of SUs. The thermal model incorporates a model of heat generation in rolling bearings, a model of heat transfer from bearings, and models for estimation of temperature and temperature deformations of SU elements. We have carried out experimental test and made quantitative evaluation of the effect of operation conditions on friction and thermal characteristics of the SUs of grinding and turning machines of typical structures. It is found out that the operation conditions make stronger effect on SU temperatures when rpm increases. A comparison between the results of analysis and experiment proves their good mutual correspondence and allows us to recommend application of the models and software developed for design and research of high-speed SUs running on rolling bearings.

Key Words : High-Speed Spindle Unit, Rolling Bearing, Thermal Model, Thermal Characteristics

1. Introduction

SU thermal properties, besides the accuracy of rotation and static and dynamic stiffness, strongly effect the accuracy of machine tool. Heating of bearings caused by friction is one of the main factors limiting SU high-speed. Practical and analytical studies prove that when increasing SU rpm, friction losses in bearings increase to high values, and this should be estimated when choosing the bearing and drive types. Thus, for example, the estimated friction losses in the bearings of SU of lathe (spindle diameter 90 mm) at 5,000 rpm

can reach 2.9 kW after temperature stabilization (Levina et al, 1989).

Modern requirements to SUs make it necessary to estimate quantitatively their thermal characteristics at early stage of development. Application of the well-known software complexes, such as I-DEAS, ANSYS, and NASTRAN, makes sense at final stage of designing, when details of structures are under consideration. The standard complexes based on application of finite element method (FEM) facilitate simulation of SU geometry, but give no opportunity to consider specific peculiarities of SU structures (particularly, the type of bearing preloading) and conditions of operation (dependencies of SU heat transfer on rpm and temperature, viscosity of bearings' lubricant on temperature, etc.). Besides, the standard software does not incorporate the models for numerical estimation of heat generation in bearings, and require a lot of preparatory work before

* Corresponding Author,
  E-mail : cmlee@sarim.changwon.ac.kr
  TEL : +82-55-279-7572; FAX : +82-55-267-5142
  Machine Tool Research Center, Changwon National University, #9 Sarimdong Changwon, Kyungnam, 641-773 Korea. (Manuscript Received September 9, 2002; Revised February 12, 2003)
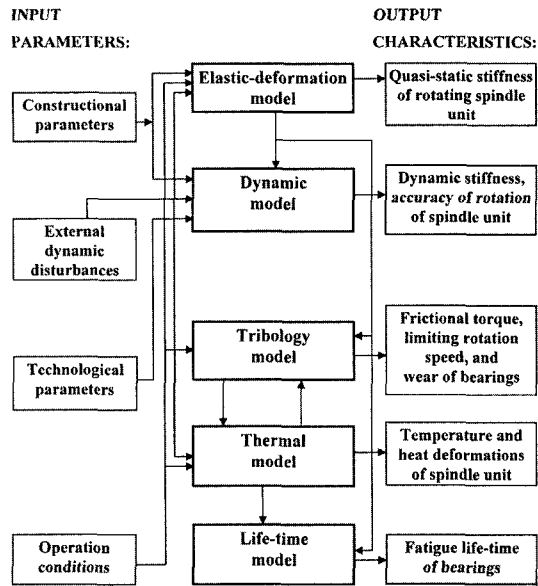
INPUT
PARAMETERS:

OUTPUT
CHARACTERISTICS:

Fig. 1 Diagram of the complex model of spindle units

usage.

That is why, following the purpose to increase quality and efficiency of SU design process at early stage, we develop a thermal model of SU and specialized software intended for numerical express-evaluation of frictional and thermal characteristics of high-speed SUs in accounting for their structural and functional peculiarities (Zverev and Push, 2000). In order to realize the model, we apply the universal beam element analytical diagrams of SUs for solution of the problems of statics, dynamics, and heat transfer of SUs (Fig. 1).

Using the software developed, we obtain the numerical evaluations of the effect of operation parameters (rpm, external load, bearing preloads, parameters of lubricant, and heat transfer) on the friction and thermal characteristics of high-speed SUs of grinding and turning machines. We also perform an experimental study of friction and thermal characteristics of a SU of grinding machine using a special rig and the standard instruments. Comparison of the results of numerical and experimental studies obtained proves high efficiency of the model and software developed.

2. Principle Statements of Thermal Analysis

Thermal model of a system 'SU - external medium' presumes estimation of the following characteristics : friction losses (heat generation) in bearings ; heat transfer from SU's surfaces ; temperatures and temperature deformations of SU's elements.

2.1 Assumptions and conditions used in thermal analysis

When developing a thermal model of SU, we make the following assumptions :

* the main source of heat generation in bearings is friction ;
* the heat generated in bearing distributes equally between inner and outer races ;
* the bearings are considered to be circular heat sources ;
* the temperatures of spindle and cylindrical housing are constant within structures' radial cross-sections.

When estimating heat generation in bearings and heat transfer from SU's elements, we assume that :

* heat generation in bearings can be determined by hydrodynamic and load components of friction ; at that, the lubricant viscosity depends on bearing temperature ;
* excessive heat dissipates by means of free and forced convective heat transfer and heat conductivity of SU's materials ;
* thermal-physical parameters of heat transfer are the functions of temperature and rate of surface air-cooling ;
* variations of clearance-tightness in bearings with temperature are the result of the differences of temperatures of SU's elements, conditions of heat transfer, and differences in the properties of materials of spindle and housing.

When developing analytical thermal diagram of SU, we use one-dimensional axial beam elements
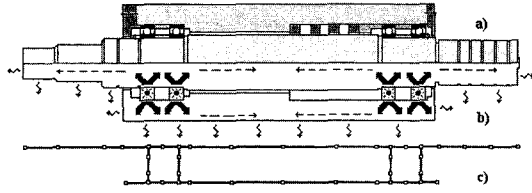
Fig. 2 Structural (a), heat transfer (b), and analytical (c) diagrams of the spindle unit

and radial ring elements. In Fig. 2, we show the diagram of heat transfer and analytical diagram of SU mounted in bush-type casing.

As a result of heat generation in bearing, its temperature increases up to the moment when the generated and transferred heat becomes equal. This condition is assumed to be a condition of heat balance (stationary heat exchange), and can be represented in the form of equation of heat balance:

$$Q_B = Q_S + Q_H + Q_C, \tag{1}$$

where Q_B is the quantity of heat generated in bearing; Q_S and Q_H are the heat outputs provided by spindle and housing, respectively; Q_C is the heat output provided by SU cooling system.

Heat generation in bearing can be determined as the function of friction losses for given conditions of SU operation:

$$Q_B = Q_B(M_F, n), \tag{2}$$

where M_F is the bearing friction torque; n is the spindle rpm.

Heat transfer from bearings takes place in axial direction along spindle and housing. Interaction of convection and radiation of heat can be estimated by the weighted average values of coefficients of heat transfer from SU's surfaces. Determination of the coefficients of heat transfer for particular conditions of SU operation makes the main difficulty of thermal analysis. The corresponding analytical dependencies of coefficients of heat transfer on temperature and rate of air-cooling of surfaces are presented in (Leontiev, 1979). The linear dependencies of coefficients of heat conductivity of SU materials on temperature (in the temperature band 20-100°C) can be obtained from the reference data presented in (Leontiev, 1979).

2.2 The model of heat generation in spindle bearings

Heat generation in bearings (friction losses) depends on many factors, estimation of which makes a complicated theoretical problem (Spitsin and Atras, 1966). Since this problem is not solved yet, we use the simplified engineering method by Palmgren (Palmgren, 1964), which gives us the following formula for bearing friction torque:

$$M_F = M_0 + M_1 \tag{3}$$

Here, M_0 is the hydrodynamic component of friction torque, which does not depend on load, but depend on rpm; M_1 is the load dependent component, which does not depend on rpm.

The friction losses N_F (in W) equal to the power of heat generation QB in bearing, we estimate by the formula:

$$N_F = Q_B = 1.047 \cdot 10^{-3} \cdot n \cdot M_F, \tag{4}$$

where the hydrodynamic component of friction torque:

$$M_0 = 10^{-7} \cdot f_0 \cdot (\nu \cdot n)^{2/3} \cdot d_m^3 \quad (\text{if } \nu \cdot n \geq 2000); \tag{5}$$
$$M_0 = 160 \cdot 10^{-7} \cdot f_0 \cdot d_m^3 \quad (\text{if } \nu \cdot n < 2000). \tag{6}$$

Here, d_m is the averaged bearing diameter in mm; $\nu(T)$ is the lubricant kinematic viscosity at the temperature T in cSt; f_0 is the coefficient dependent on lubricant type (see Table 1).

The load dependent component of friction torque:

$$M_1 = f_1 \cdot P \cdot \left(\frac{P}{C_0}\right)^c \cdot d_m; \quad \text{(for ball bearings)} \tag{7}$$

$$M_1 = f_1 \cdot P \cdot d_m, \quad \text{(for roller bearings)} \tag{8}$$

Here, P is the equivalent load applied to the bearing in dN; C_0 is the bearing static load carrying capacity in dN; c and f_1 are the coefficients dependent on type of bearing and character of loading (see Table 1).

The equivalent load can be estimated as follows:

$$P = 0.9 \cdot P_a \cdot ctg(\alpha) - 0.1 \cdot P_r; \quad \text{(for ball bearings)}; \tag{9}$$
$$P = 0.8 \cdot P_a \cdot ctg(\alpha) ; \quad \text{(for taper roller bearings)}; \tag{10}$$
$$P = P_r, \quad \text{(for cylindrical roller bearings)}, \tag{11}$$

where P_a and P_r are the axial and radial loads; α is the bearing contact angle.

Table 1 Factors f_0, f_1, and c

Bearings	Type of lubrication factor f_0					Bearing loading factor f_1	Bearing type factor c
	Oil-Air	Grease	Oil-Injection	Oil-Circulation	Oil-Drop		
Double-row cylindrical roller bearing	1.5-3	3-4	6-10	8-12	2-4	0.00025	0
One-row taper roller bearing	1.5-2	1.5-4	6-8	8-10	1.5-3	0.0005	0
One-row angular ball bearing	0.7-1	0.7-2	3-4	4-5	0.7-1	0.002	0.5
Double-row angular ball bearing	1.4-2	1.5-4	6-8	8-10	1.4-2	0.002	0.33
Double-row taper roller bearing	3-4	3-6	12-16	16-20	3.5-6	0.001	0

In the case of double-row cylindrical roller bearing, we specify the friction losses by taking into account the bearing real clearance-tightness following the experimental results presented in (Figatner, 1967). For this purpose, we introduce the coefficient k_r into the formula (8), which takes into account the real radial clearance-tightness Δ_r (μm), which varies with temperature and depends on thermal deformations of bearing's elements:

$$k_r = 2 - 10^4 \cdot \frac{\Delta_r}{d_s}; \quad \text{(clearance)} \qquad (12)$$

$$k_r = 0.26 \cdot \left(2 + 10^4 \cdot \frac{|\Delta_r|}{d_s}\right)^3, \quad \text{(tightness)} \quad (13)$$

where d_s is the spindle's journal diameter in mm.

Variation of hydrodynamic component of friction losses in bearing M_0 depends on the coefficient f_0. In order to facilitate engineering analysis, we propose to use the limiting values of f_0 for different types of bearing lubrication (see Table 1), which we obtained by generalization of the results of different studies (Spitsin and Atras, 1966; Gan and Zaitov, 1988). At low and moderate loads applied to SU, the idle friction torque M_0 makes the greatest part (up to 85-95%) of the total bearing friction torque. However, the

components M_0 and M_1 interfere, since when the load increases, an increase of the load component M_1 brings to an increase of the temperature, which, in turn, causes a decrease of lubricant viscosity, and, thus, a decrease of the hydrodynamic component M_0.

In practice, SU thermal characteristics can vary significantly, and this variation is caused by a number of factors effecting conditions of heat generation and transfer. Particularly, a significant effect makes the variations of lubricant viscosity and volume. When evaluating heat generation in bearings, we estimate the dependence of oil viscosity ν on temperature T (for the temperature band 20-150°C) using the following power dependence (Leontiev, 1979):

$$\nu(T) = \nu_{40} \cdot \left(\frac{40}{T}\right)^m, \qquad (14)$$

where ν_{40} is the kinematic viscosity (in cSt) at 40°C, m is the exponent.

Following the results obtained in Russian Scientific Research Institute for Machine Tools (ENIMS) (Dzuba, 1985) and applying the graphic 'viscosity - temperature' proposed by FAG Company (Brandlein, 1985), we can estimate the exponent 'm' by the formula:

$$m=\frac{\ln\left(\frac{\nu_2}{\nu_1}\right)}{\ln\left(\frac{T_1}{T_2}\right)},\qquad(15)$$

where subscripts 1 and 2 denote the upper and lower values of temperature and viscosity of lubricant in the operation band, respectively.

2.3 Equation of heat transfer and solution method

A solution of the nonstationary problem of heat transfer can be derived by applying FEM and solving the system of linear differential equations in the matrix form (Segerlind, 1976):

$$\mathbf{C}\cdot\dot{\boldsymbol{T}}+\mathbf{H}\cdot\boldsymbol{T}=\boldsymbol{Q}(\mathrm{t}),\qquad(16)$$

where $\mathbf{C}$ and $\mathbf{H}$ are the matrices of heat capacity and heat conductivity of SU; $\boldsymbol{T}$ is the vector of unknown node temperatures; $\boldsymbol{Q}$ is the vector of heat load; t is time.

The matrices of heat capacity and heat conductivity, we represent as follows:

$$\mathbf{C}=\sum_{e=1}^{p}\mathbf{C}_e\,;\ \mathbf{H}=\sum_{e=1}^{p}\mathbf{H}_e,\qquad(17)$$

where $\mathbf{C}_e$ and $\mathbf{H}_e$ are the local matrices of heat capacity and heat conductivity of the element 'e'; p is the number of elements in SU analytical diagram. For the axial beam type and radial elements (see Fig. 2), we obtain the expressions for local matrices of heat conductivity and heat capacity using the general integrals of FEM (Segerlind, 1976). Thus, for a beam type element, we have:

$$\mathbf{H}_e^{b}=\int_{V_e}\mathbf{B}^T\cdot\mathbf{D}\cdot\mathbf{B}\cdot dV+\int_{S_2}h_2\cdot\mathbf{N}^T\cdot\mathbf{N}\cdot dS_2+\int_{S_1}h_1\cdot\mathbf{N}^T\cdot\mathbf{N}\cdot dS_1$$
$$=\frac{\eta\cdot S_1}{L}\cdot\begin{bmatrix}1 & -1\\-1 & 1\end{bmatrix}+\frac{1}{6}\cdot P\cdot L\cdot h_2\cdot\begin{bmatrix}2 & 1\\1 & 2\end{bmatrix}+h_1\cdot S_1\cdot\begin{bmatrix}1 & 0\\0 & 1\end{bmatrix};\qquad(18)$$

$$\mathbf{C}_e^{b}=\frac{1}{6}\cdot\rho\cdot c\cdot S_1\cdot L\cdot\begin{bmatrix}2 & 1\\1 & 2\end{bmatrix},\qquad(19)$$

where V_e is the element volume; S_1, S_2, and h_1, h_2 are the areas and heat-transfer coefficients of the face and side surfaces of the element, respectively; L is the column length; P is the perimeter of column cross-section; η, ρ, and c are the coefficients of heat-conductivity, density, and specific heat capacity of material, respectively.

For elemental annulus, we have:

$$\mathbf{H}_e^{r}=\frac{2\pi}{3}\cdot\eta\cdot\frac{R_j{}^3-R_i{}^3}{(R_j-R_i)^2}\cdot\begin{bmatrix}1 & -1\\-1 & 1\end{bmatrix}$$
$$+2\pi\cdot R_j\cdot\delta\cdot h_1\cdot\begin{bmatrix}0 & 0\\0 & 1\end{bmatrix}+2\pi\cdot R_i\cdot\delta\cdot h_2\cdot\begin{bmatrix}1 & 0\\0 & 0\end{bmatrix};\qquad(20)$$

$$\mathbf{C}_e^{r}=\frac{\pi\cdot\rho\cdot c}{30\cdot\delta^2}$$
$$\cdot\begin{bmatrix}2R_j{}^5-20R_j{}^2R_i{}^3+30R_jR_i{}^4-12R_i{}^5 & 3R_j{}^5-5R_j{}^4R_i+5R_jR_i{}^4-3R_i{}^5\\ 3R_j{}^5-5R_j{}^4R_i+5R_jR_i{}^4-3R_i{}^5 & 12R_j{}^5-30R_j{}^4R_i+20R_j{}^3R_i{}^2-2R_i{}^5\end{bmatrix};\qquad(21)$$

where R_j and R_i are the element external and internal radiuses; δ is the element thickness; h_1 and h_2 are the heat-transfer coefficients at external and internal surfaces of the element, respectively.

The equation system (16) can be solved using the finite difference method and applying the unconditionally stable central-difference diagram (Forsythe et al, 1977). In order to do this, we replace the derivative in (16) by its approximate finite-difference analogue $\dot{\boldsymbol{T}}\approx(\boldsymbol{T}_{i+1}-\boldsymbol{T}_i)/\Delta t$. Here, $\boldsymbol{T}_i$ and $\boldsymbol{T}_{i+1}$ are the values of temperature vector in the instants of time t_i and t_{i+1}; Δt is the integration step in time. Then, the equation system (16) takes the following form:

$$(\mathbf{H}+\frac{2}{\Delta t}\cdot\mathbf{C})\cdot(\boldsymbol{T}_i+\boldsymbol{T}_{i+1})=\frac{4}{\Delta t}\cdot\mathbf{C}\cdot\boldsymbol{T}_i+(\boldsymbol{Q}_i+\boldsymbol{Q}_{i+1}).\qquad(22)$$

The system (22) can be solved by step-by-step calculations within the time interval under consideration. At that, for each time step, we determine the matrix $\mathbf{H}$ and the vector $\boldsymbol{Q}$ following the conditions of previous step, and this gives us an opportunity to specify and vary the conditions of uniqueness of solution (heat-transfer coefficients, load, rpm, and lubricant viscosity) in time.

Having the results of temperature analysis, we can start estimation of temperature deformations of SU's elements. Thus, we calculate temperature elongation ΔL of each one-dimensional element (column type or radial) using the formula:

$$\Delta L=\varepsilon\cdot L\cdot\Delta T,\qquad(23)$$

where L is the initial linear dimension of the element under consideration, ε is the linear expansion coefficient, ΔT is the element excessive temperature.

Variations of clearance-tightness in bearings with temperature are caused by the non-uniform heating and differences in linear expansion coefficients of materials of SU's elements. Thus, variation with temperature of the radial clearance-tightness Δ_r in cylindrical roller bearing can be determined from the balance of displacements :

$$\Delta_r = \Delta d_1 - \Delta d_2 + \Delta d_3 - \Delta d_4 - \Delta d_5, \qquad (24)$$

where Δd_1 is the thermal expansion of housing bush ; Δd_2 is the thermal expansion of spindle's journal ; Δd_3 and Δd_4 are the thermal expansions of bearing's outer and inner rings, respectively ; Δd_5 is the thermal expansion of rolling bodies (balls or rollers). The temperature deformations Δd_1, Δd_2, Δd_3, Δd_4, and Δd_5 can be calculated using the formula (23).

2.4 Algorithm of thermal analysis

In Fig. 3, we present a flow chart of algorithm for SU thermal analysis, which incorporates the following main procedures. In blocks 1 and 2, we introduce the vector of initial temperature T_0, the duration of thermal process τ, and the integration time step Δt, and calculate the matrices of heat capacity **C** and heat conductivity **H** of SU by summation of the local matrices.

In block 3, we calculate the vector of SU heat load $\boldsymbol{Q}$ (the power of heat generation in bearings) as a function of the vector of current temperature T. The algorithm of bearing temperature analysis is of iteration type, since bearing temperature depends on heat generation in bearings, which, in turn, depends on the temperature via lubricant viscosity, i.e., $\boldsymbol{Q} = \boldsymbol{Q}(\nu)$ and $\nu = \nu(T)$. Heat balance, as we mentioned in Sec. 2.1, takes place when heat generation equals heat transfer in bearings. In general case, in order to estimate both of these components, we need to introduce some initial temperature. In Fig. 4, we present in general the process of successive approximation to the searched bearing's temperature T_B, starting from some initial T_0.

In block 4, we solve the equation of SU heat conductivity (16) reduced to the form (22), and determine the vector of node temperatures T. Besides, in the cycle, where we determine the
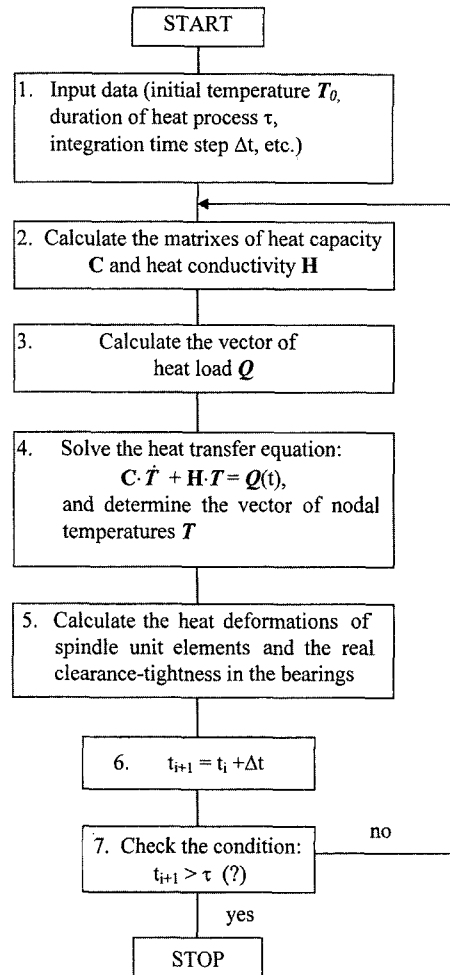

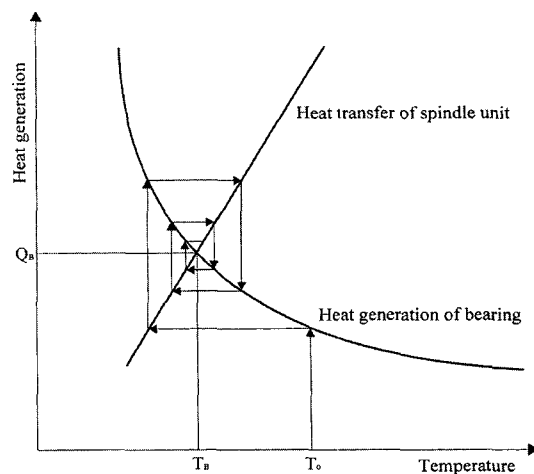**Fig. 3** Algorithm diagram of the thermal problem solution

Fig. 4 Heat balance in bearings

temperature in dependence from lubricant viscosity, we check the condition of iteration process conversion. In order to do this, we calculate the absolute values of temperature differences at current and previous steps of iteration for each bearing. We assume that bearing temperature stabilizes, when the temperature difference dose not exceed 0.1°C. Our experience of computations proves that the estimated temperature stabilizes after 5-7 iterations, assuming that the initial temperature of the bearings is equal to the temperature of the environment.

Then, in block 5, knowing the temperatures T, we calculate the temperature deformations of SU's elements and the temperature variations of clearance-tightness in bearings.

In block 6, we switch to another time interval $t_{i+1}=t_i+\Delta t$. In block 7, we check whether the process has reached the given time τ. If this condition is satisfied, we stop computations. If not, we recalculate the power of heat generation in SU's bearings for the next time interval in accounting for the values of temperature and clearance-tightness in bearings calculated at previous step, and then, solve again the equation of SU heat conductivity (block 4) and determine the thermal characteristics of SU.

3. Investigation of Friction and Thermal Properties

Using the algorithms and software developed, we made the numerical studies of friction and thermal properties of the SUs of grinding and turning machines and compared the results with those obtained in experimental studies. At that, we studied the effect of operation conditions (rpm, axial preload of bearings, external load, conditions of heat transfer from SU's surfaces, type of bearing lubrication, and lubricant viscosity) and checked the validity of mathematical models and software developed.

The experimental study of a grinding machine's SU (Fig. 2) we carried out using a rig presented in Fig. 5.

The SU was mounted in the air bearing designed for measurements of the bearing friction
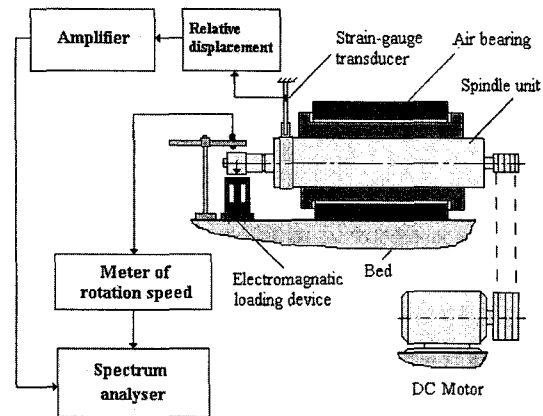

Fig. 5 Layout of the experimental rig

torque using a thread, one end of which was attached to a strain-gauge transducer, and the other one to the SU's housing. The strain-gauge transducer signal was amplified by KWS-73 (Hettynger Co) and, then, inputted to the spectrum analyser 2031 (B&K Co.). The spindle was rotated by a belt drive using DC motor. The spindle was constantly and radially loaded by a contactless electromagnetic loading device. The SU bearings were axially preloaded with the help of a calibrated spring and a special screw device in the housing to adjust a variable number of working spring coils. The SU temperature we measured using a contact type thermometer (SKF Co.), which provided the accuracy of temperature measurements within ±1°C in the temperature band from −40 to +120°C. In order to measure the temperature of the front bearing, the SU's housing was drilled through, and the temperature gauge was placed inside the hole. The bearings were lubricated by grease NBU15 (Kluber Co.) having viscosity 13.7 cSt at 40°C. Before the tests, the SU was run-in at 5,000 rpm at idle for 4 hours (Fig. 6).

From Fig. 6(a) it follows that in process of run-in and lubricant mixing, the lubricant viscosity decreases with temperature, and the friction torque decreases approximately in 2.5 times during the first 1.5-2 hours of SU operation. The bearing temperature stabilization takes place approximately at the same time (Fig. 6(b)).
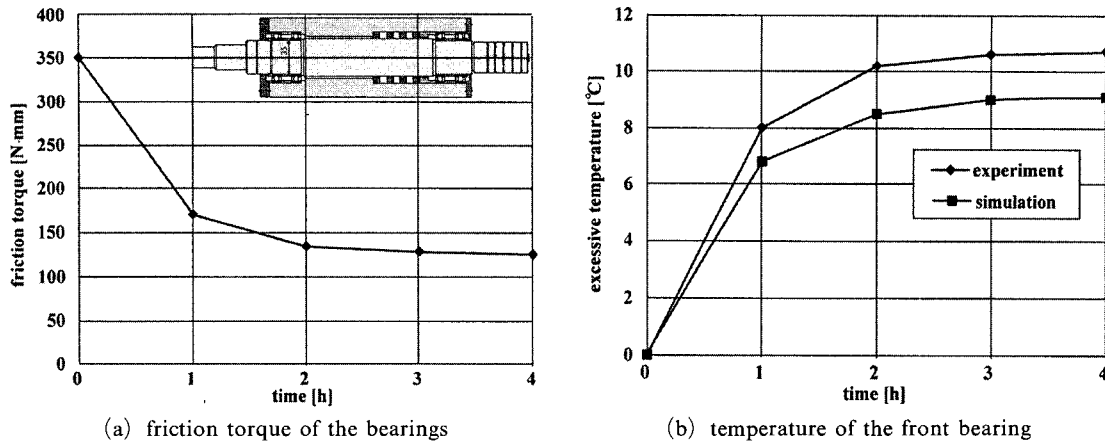
The dependencies of stabilized total friction

(a) friction torque of the bearings

(b) temperature of the front bearing

Fig. 6 Aggregate friction torque (a) and temperature (b) in time

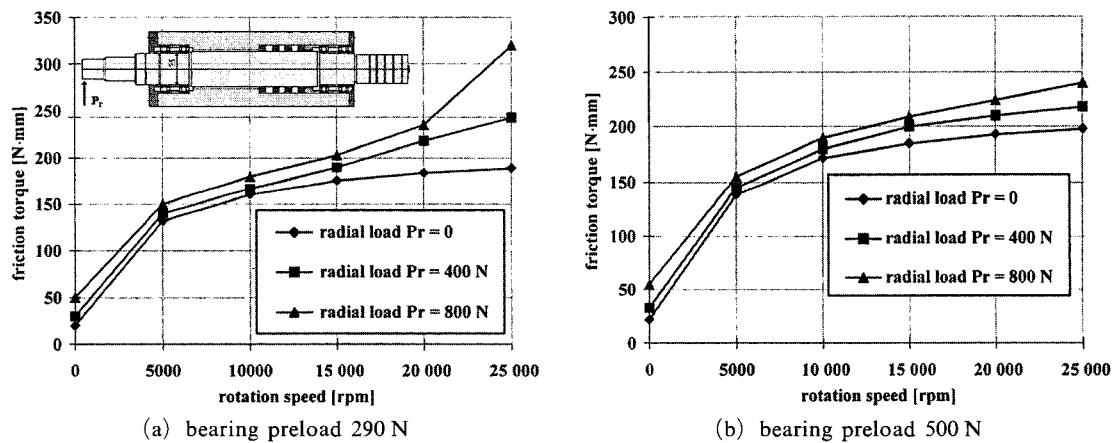(a) bearing preload 290 N

(b) bearing preload 500 N

Fig. 7 Experimental aggregate friction torque of the bearings related to rpm

torque of SU's bearings on rpm and radial load P_r are presented in Fig. 7(a) (for the bearing axial preload 290 N).

It follows that at idle $(P_r=0)$, an increase of rpm brings to decrease of the torque increment (which is caused, besides the other reasons, by an increase of temperature and decrease of lubricant viscosity), and this does not happen when the spindle is heavy loaded in radial direction $(P_r= 800 \text{ N})$. We explain it by the fact that an additional radial loading of high-speed SU brings to loose contacts of a part of bearing's balls with the races, and, thus, to gyroscopic sliding of the balls that increases the friction losses (hydrodynamic component of friction torque). When increasing the bearing preload up to 500 N, the destabilizing effect of radial load on friction torque decreases,

because the preload increases the loads at balls' contacts and eliminates gyroscopic sliding (Fig. 7 (b)).

In Fig. 8, we present the dependencies of estimated friction torque (Fig. 8(a)) and the calculated and measured temperatures of SU's front bearing (Fig. 8(b)) on rpm (at idle, i.e., when $P_r=0$, for the axial preload 290 N). We can see that the dependence of bearing temperature on rpm is close to linear. The maximal relative error of bearing temperature calculation at the maximum 25,000 rpm makes 13.5%, and this can be considered to be a satisfactory result in engineering analysis.

From contact-hydrodynamic theory of lubrication (Kodnir, 1976) it follows that lubricant viscosity and amount, as well as the type of lubri-
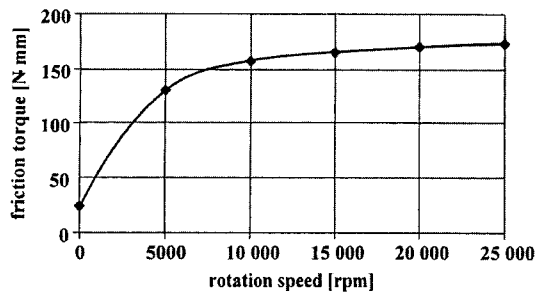
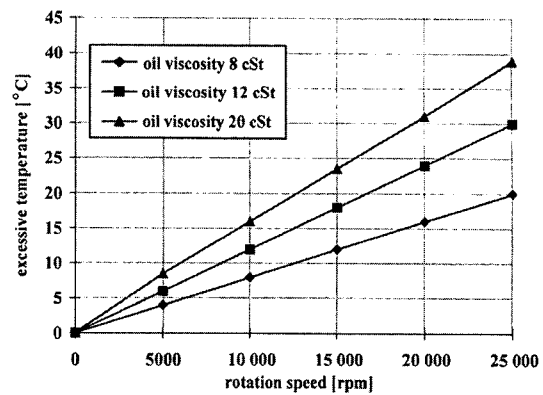(a) friction torque of the bearings
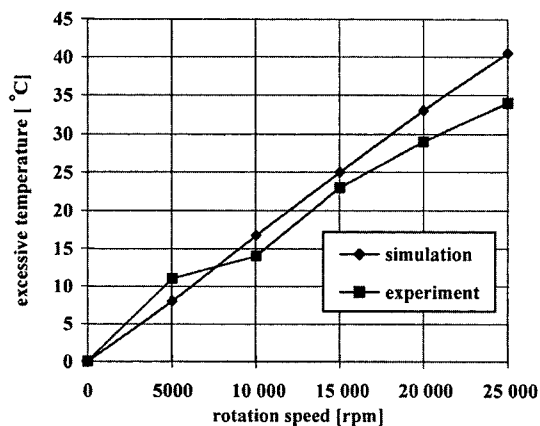
(b) temperature of the front bearing

Fig. 8 Aggregate friction torque (a) and temperature (b) related to rpm

(a) effect of lubricant viscosity

(b) effect of lubrication type

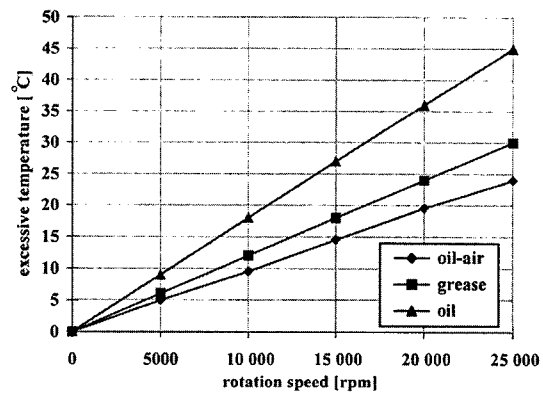**Fig. 9** Temperature of the front bearing related to rpm

cation, significantly influence the friction losses in rolling bearings. That is why improving the parameters and systems of bearing lubrication at present is one of the principle means to increase SU high-speed (Dzuba, 1985).

In Fig. 9(a), we present the results of numerical estimation of the effect of oil viscosity on SU's ball bearing temperature. In Fig. 9(b), we present the results of estimation of the effect of lubrication type on the SU's bearing maximum temperature.

From Fig. 9 it follows that the effect of lubricant parameters on bearing temperature increases with increase of rpm. Thus, variation in lubricant viscosity brings about more serious variation in temperature at high rpm (see Fig. 9(a)). We can see that at 25,000 rpm (Fig. 9(b)), SU lubrication with oil-mist (oil-air mixture) reduces the bearing temperature approximately in two times with respect to lubrication with oil. The lubricant

volume should be adjusted with rpm to minimize excessive heating. A numerical evaluation of the efficiency of so-called 'minimum' lubrication is presented in (Smirnov, 1979).

The bearing temperature is greatly influenced by the factor of convective heat transfer from SU's surfaces. Our analysis proves that at low rpm spindle accepts approximately 20-30% of heat generated in bearings. At high rpm, this figure increases up to 45-55% because of the increase (in the power 0.7) of heat transfer from the open rotating air-cooled surfaces. When making numerical experiments (as shown in Fig. 10), we varied the heat-transfer coefficient of SU housing of grinding machine within $20\ W \cdot (m^{-2} \cdot {}^{\circ}C^{-1})$ (that is typical for natural cooling) and $200\ W \cdot (m^{-2} \cdot {}^{\circ}C^{-1})$ (that is typical for forced cooling).

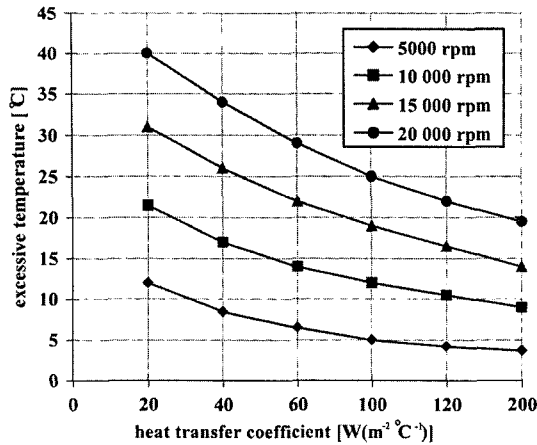The results of analysis show that a significant

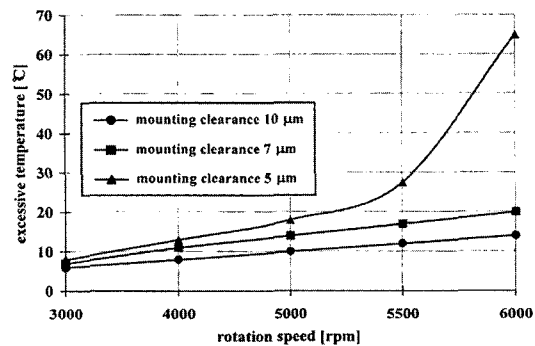Fig. 10 Temperature of the front bearing related to heat transfer coefficient

increase of heat transfer from the housing surface can bring about decrease of bearing temperature by 7-8°C at the relatively low rpm (5,000 rpm) and by 20-22°C at the high rpm (20,000 rpm). At that, the share of heat transferred by the housing increases up to 80%. A general analysis that we made to study the heat transfer conditions proves high efficiency of this method to bearing temperature decrease.

In SUs with double-row roller bearings, the character of dependence of temperature on rpm can turn to be non-linear. In the SU assembly, a mounting radial clearance in double-row roller bearings should be provided. At that, when the rpm increases, and the heat generated in bearings increases, as well, a non-uniform heating of the housing and spindle usually brings to a decrease of clearance, which can transform to tightness (Fig. 11(a)). When the tightness appears, the friction losses in bearing increase drastically (according to the formula (13), the dependence has the power 3), and the temperature increases (see Fig. 11(b)) too.

The temperature increase with rpm has a dual character. If in the result of heating the clearance does not transform into the tightness, the dependence of temperature on rpm keeps linear, but if the transform takes place, the temperature increases drastically. In Fig. 11, we can see that it happens at 5,500 rpm (if the mounting clearance is 5 μm). The transformation of clearance into
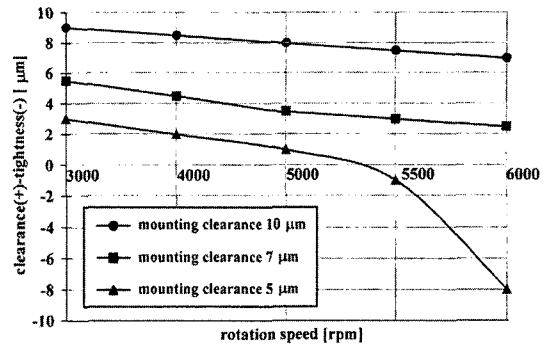
(a) clearance-tightness of the front roller bearing

(b) temperature of the front roller bearing

Fig. 11 Real clearance-tightness (a) and temperature (b) related to rpm

tightness in SU's bearings, in turn, can bring to the changes of elastic-deformation and dynamic properties of SU (see Fig. 1). Thus, the mounting clearance in rolling bearings operating at high rpm should be chosen based on preliminary analysis, and this is of great practical importance. Availability of the SU thermal model even gives us an opportunity to simulate and predict heat 'seizure' in cylindrical roller bearings, which can be caused by a drastic increase of friction losses and temperature in result of the transformation clearance-tightness.

4. Conclusions

(1) Having a purpose to improve quality of designing of high-speed SUs on rolling bearings, we have developed a SU thermal model, which is one element of a SU complex model. We represented the thermal model as software for express analysis of SUs at the initial stage of

designing. The thermal model incorporates a model of heat generation in bearings, a model of heat transfer from bearings, and the models for evaluation of temperature and temperature deformations of SU elements. The model is based on application of beam type finite element analytical diagrams of SUs to apply them for solution of problems of statics, dynamics, and heat conduction, which is of a great importance for practical realization of our complex approach to simulation of SUs in designing.

(2) We have made the experimental studies and the numerical estimations of the effect of operation conditions on the friction and thermal properties of SUs of grinding and turning machines. We found out that the dependence of ball bearing temperature on rpm is approximately linear. In the SUs running on double-row roller bearings in the case of small preliminary radial clearance, an increase of rpm can bring to a temperature 'jump' caused by a transformation of clearance into tightness followed by drastic increase of heat generation in the bearing. Under minor external loads, an increase of rpm brings to a decrease of friction torque increment, but this does not happen under significant external radial loads and low preloads in ball bearings. The effect is caused by unloading a part of balls in the bearing loaded by heavy radial force, and the ball gyroscopic sliding followed by an increase of friction losses. The lubricant parameters and the parameters of SU cooling make stronger effect on bearing temperature when rpm increases. The comparisons of the results of calculations and tests made prove efficiency of the thermal model and its applicability for SU design.

Acknowledgment

References

Brandlein, K., 1985, "Machining Spindle and Its Bearings," Proceedings of the symposium of FAG Company, Moscow Research Institute of Machine Tools, Russia, pp. 52~78.

Dzuba, V. I., 1985, Effective lubricant systems for high-speed spindle units on rolling bearings, Ph. D. thesis, Moscow Research Institute of Machine Tools, Russia.

Figatner, A. M., 1967, "The Effect of Radial Clearance-Tightness of Roller Bearings of Precise Spindle units," *Journal of Machines & Cutting Tools*, 2, pp. 15~18.

Forsythe, G., Malcoln, M. and Moler, C., 1977, *Computer Methods for Mathematical Computations*, Prentice-Hall, Englewood Cliffs, New Jersy.

Gan, K. G. and Zaitov, L. M., 1988, "Dependence of Friction Torque of High-Speed Ball Bearing on Rotation Speed and Axial Preloading," *Bulletin of Machine Industry*, 11, pp. 21~23.

Kodnir, D. S., 1976, *Contact Hydrodynamics of Lubrication*, Mashinosrtoenie, Moscow.

Smirnov, A. I., 1979, "Optimisation of Lubrication Systems of High-Speed Spindle Units," Proceedings of Moscow Engineering Research Institute, Russia, pp. 3~69.

Leontiev, A. I., 1979, *The Theory of Heat Interchange*, Moscow : High School, Russia.

Levina, Z. M., Gorelik, I. G., Zverev, I. A. and Segida, A. P., 1989, "Computer Analysis of Elastic-Deformation, Dynamic, and Temperature Characteristics of Spindle Units at Designing, Proceedings of Moscow Research Institute of Machine Tools, Russia, pp. 3~89.

Palmgren, A. C., 2000, Grundlage der Waelzlagertechnik, Stuttgart, Germany.

Segerind, L. J., 1976, *Applied Finite Element Analysis*, John Wiley & Sons Inc., N-Y/London/Sydney/Toronto.

Spitsin, N. A. and Atras, S. G., 1966, Friction losses in rolling bearings, Proceedings of Moscow Institute of Bearing Industry, Russia, pp. 121~130.

Zverev, I. A. and Push, A. V., 2000, *Spindle Units : Quality and Reliability at Designing*, Moscow State University of Technology Press, Russia.